

Multiple temperature kinetic model and gas-kinetic method for hypersonic non-equilibrium flow computations

Kun Xu^{a,*}, Xin He^b, Chunpei Cai^c

^a *Mathematics Department, Hong Kong University of Science and Technology, Hong Kong*

^b *China Aerodynamics Research and Development Center, Sichuan, China*

^c *ZONA Technology Inc., Scottsdale, AZ 85251, USA*

Received 18 December 2007; received in revised form 17 March 2008; accepted 23 March 2008

Available online 8 April 2008

Abstract

It is well known that for increasingly rarefied flowfields, the predictions from continuum formulation, such as the Navier–Stokes equations lose accuracy. For the high speed diatomic molecular flow in the transitional regime, the inaccuracies are partially attributed to the single temperature approximations in the Navier–Stokes equations. Here, we propose a continuum multiple temperature model based on the Bhatnagar–Gross–Krook (BGK) equation for the non-equilibrium flow computation. In the current model, the Landau–Teller–Jeans relaxation model for the rotational energy is used to evaluate the energy exchange between the translational and rotational modes. Due to the multiple temperature approximation, the second viscosity coefficient in the Navier–Stokes equations is replaced by the temperature relaxation term. In order to solve the multiple temperature kinetic model, a multiscale gas-kinetic finite volume scheme is proposed, where the gas-kinetic equation is numerically solved for the fluxes to update the macroscopic flow variables inside each control volume. Since the gas-kinetic scheme uses a continuous gas distribution function at a cell interface for the fluxes evaluation, the moments of a gas distribution function can be explicitly obtained for the multiple temperature model. Therefore, the kinetic scheme is much more efficient than the DSMC method, especially in the near continuum flow regime. For the non-equilibrium flow computations, i.e., the nozzle flow and hypersonic rarefied flow over flat plate, the computational results are validated in comparison with experimental measurements and DSMC solutions.

© 2008 Elsevier Inc. All rights reserved.

Keywords: Multiple temperature kinetic model; Gas-kinetic method; Hypersonic and rarefied flows

1. Introduction

The development of aerospace technology has generated a strong demand on research associated with rarefied gas dynamics. The classification of the various flow regimes based on the dimensionless parameter, the Knudsen number, is a measure of the degree of rarefaction of the medium. The Knudsen number Kn is defined

* Corresponding author. Tel.: +852 2358 7443; fax: +852 2358 1643.

E-mail address: makxu@ust.hk (K. Xu).

as the ratio of the mean free path to a characteristic length scale of the system. In the continuum flow regime where $Kn < 0.001$, the Navier–Stokes equations with linear relations between stress and strain and the Fourier’s law for heat conduction are adequate to model the fluid behavior. For flows in the continuum-transition regime ($0.01 < Kn < 1$), the Navier–Stokes equations are known to be inadequate. This regime is important for many practical engineering problems, such as the simulation of microscale flows and hypersonic flow around space vehicles in low earth orbit [11,13]. Hence, there is a strong desire and requirement for accurate models which give reliable solutions with lower computational costs. The Boltzmann equation describes the flow in all flow regimes; continuum, continuum-transition and free molecule motion.

The numerical techniques available for solving the Boltzmann equation can be classified into particle methods and continuum methods. The direct simulation Monte Carlo (DSMC) [5] falls in the category of particle methods. The DSMC method is a widely used technique in the numerical prediction of low density flows. However, in the continuum-transition regime, where the density is not low enough, the DSMC requires a large number of particles for accurate simulation, which makes the technique expensive both in terms of the computation time and memory requirement. At present, the accurate modeling of realistic configurations, such as aerospace vehicles in three dimensions by the DSMC method for $Kn \ll 1$, is beyond the currently available computing power. Alternative methods, which solve the Boltzmann or model equations directly with the discretization of the phase space [1], have attracted attentions in recent years. But, its efficiency may be even inferior in comparison with DSMC method.

Among continuum solution methodologies, there are primarily two approaches: the Chapman–Enskog method [8], and the method of moments [10]. In the Chapman–Enskog method, the phase density is expanded in powers of the Knudsen number, where the zeroth-order expansion yields the Euler equations, the first-order results in the equations of Navier–Stokes and Fourier, the second order gives the Burnett equations, and the third order expansion presents the so-called super-Burnett equations. It is well recognized that the equations of Navier–Stokes and Fourier cease to be accurate for Knudsen number above 0.1, and one might theorize that the Burnett and Super-Burnett equations are valid for larger Knudsen numbers. Unfortunately, the higher-order equations are shown to be linearly unstable for processes involving small wavelengths, or high frequencies, and thus cannot be used in numerical simulations [6]. In recent years, several authors presented augmented forms of the Burnett equations containing additional terms of the super-Burnett order as a way of stabilizing the Burnett equations [33], the BGK–Burnett equations [3], or the regularized hyperbolic equations through relaxation, reproducing the Burnett equations when expanded in Kn [12].

In the method of Grad, the Boltzmann equation is replaced by a set of moment equations which are the first order partial differential equations for the moments of the distribution function. The actual number of moments needed depends on the process being considered, but experience shows that the number of moments had to be increased with increasing Knudsen number [17]. Since the moment equations are hyperbolic, the Grad method leads to a shock structure with spurious sub-shocks for Mach numbers greater than 1.65 for the 13 moment equations [27]. It is interesting to note that a close connection between the Grad’s moments method and the Burnett and Super-Burnett equations has been established [24]. Further, Struchtrup and Torrilhon regularized Grad’s 13 moment equations with the help of the Burnett equations and successfully applied the method to the shock structure computation up to Mach 3 of a monatomic gas [25]. However, at the current stage of research, a systematic development of a continuum method for monatomic and diatomic gas for the highly non-equilibrium flow is not in place. Among the Chapman–Enskog method and the method of moments, for the diatomic gas a single temperature is usually assumed, which can be inappropriate for the high speed flow in the near continuum regime. Both the experimental measurements and DSMC solutions confirmed that the multiple temperatures exist, and their effect on the thermal non-equilibrium may be significant. With the inclusion the multiple temperatures, the macroscopic Navier–Stokes governing equations have to be reformulated. As shown in this paper, the second viscosity term in NS is replaced by the translation and rotational temperature relaxation term.

At the current stage, the DSMC technique may be the only method of which the numerical solutions have good agreement with experimental measurements in the rarefied flow regime. However, the DSMC method is computationally expensive in the transition regime where conventional continuum models break down. Thus, there is impetus to develop a continuum model for these flows. Also, the continuum variables have macroscopic physical meaning and therefore, the governing equations give better insight into the behavior of the

flow. As realized by experiment and DSMC calculations, the thermal non-equilibrium with different translational and rotational temperatures appears in the near continuum flow. But, the current continuum formulations characterize the translational and rotational energy for the gas with a single temperature, which cannot correctly represent these flows.

The goal of this study is to extend the Bhatnagar–Gross–Krook (BGK) model to incorporate multiple temperatures and develop a gas-kinetic scheme based on the continuous particle distribution function for low density rarefied gas simulations. The current approach is a multiscale method. On the one hand, the gas-kinetic equation is solved for the local solution around a cell interface. On the other hand, the fluxes from the microscopic gas evolution feeds back into the finite volume method for the update of macroscopic variables. Due to the coupling of the micro–macro-scale formulation, the flow physics can be easily implemented on the microscopic level. At the same time, the scheme becomes efficient due to the update of macroscopic variables. For example, on the kinetic level the interaction between the gas and solid surface can be formulated through the particle incident and reflection from the boundary, and the velocity and temperature slips can be automatically obtained. The kinetic model developed in the present study will be applied to solve non-equilibrium nozzle flow and high speed flow over a flat plate, where both experimental measurements and DSMC solutions are available. In the continuum flow regime, our kinetic scheme goes back automatically to the BGK–NS method [28], which solves the Navier–Stokes equations accurately [32]. In the near continuum and transition regime with small Knudsen number, the multiple temperature non-equilibrium effect appears automatically due to the insufficient particle collision to equalize the temperatures. Also, our kinetic method has the similar efficiency as the standard Navier–Stokes flow solver. In what follows, Section 2 provides details on the construction of the current kinetic model and Section 3 presents the numerical method for solving this model. This is followed by the results and discussion of the non-equilibrium flow calculations presented in Section 4. The final section is the conclusion.

2. Gas-kinetic models and macroscopic governing equations for diatomic gas

In the current paper, we are going to present the kinetic model and its derived macroscopic equations in two dimension for diatomic gases. The experiments and computations presented in Section 4 are either 3D anti-symmetric or purely two-dimensional flows.

2.1. Equilibrium translational and rotational temperature model

The Boltzmann equation expresses the behavior of a many-particle kinetic system in terms of the evolution equation for a single particle gas distribution function. The simplification of the Boltzmann equation given by the BGK model is formulated as [2],

$$\frac{\partial f}{\partial t} + u \frac{\partial f}{\partial x} + v \frac{\partial f}{\partial y} = \frac{g - f}{\tau}, \quad (1)$$

where f is the number density of molecules at position (x, y) and particle velocity (u, v) at time t . The left hand side of the above equation represents the free streaming of molecules in space, and the right side denotes the collision term. If the distribution function f is known, macroscopic variables, such as mass, momentum, energy and stress, can be obtained by integration over the moments of molecular velocity. In the BGK model, the collision operator involves simple relaxation from f to a local equilibrium state g with a characteristic time scale τ . The equilibrium state is given by a Maxwellian,

$$g = \rho \left(\frac{\lambda}{\pi} \right)^{\frac{K+2}{2}} e^{-\lambda((u-U)^2 + (v-V)^2 + \xi^2)},$$

where ρ is the density, (U, V) are the macroscopic fluid velocity, and λ is the inverse of gas temperature, i.e., $\lambda = m/2kT$. Here m is the molecular mass, k is the Boltzmann constant, and T is the temperature. For an equilibrium flow, the internal variable ξ accounts for the z -direction translational and rotational modes, such as $\xi^2 = \xi_1^2 + \xi_2^2 + \dots + \xi_K^2$, and the total number of degrees of freedom K is related to the specific heat

ratio γ . In the current paper, we consider diatomic gas which has $K = 3$ with one translational mode in z -direction and two rotational degree of freedom. The relation between mass ρ , momentum $(\rho U, \rho V)$, and energy densities ρE with the distribution function f is

$$\begin{pmatrix} \rho \\ \rho U \\ \rho V \\ \rho E \end{pmatrix} = \int \psi_x f \, du \, dv \, d\xi, \tag{2}$$

where ψ_x is the component of the vector of moments

$$\psi = \left(1, u, v, \frac{1}{2}(u^2 + v^2 + \xi^2) \right)^T,$$

and the volume element in the phase space with $d\xi = d\xi_1 d\xi_2, \dots, d\xi_K$. Since mass, momentum and energy are conserved during particle collisions, f and g satisfy the conservation constraint,

$$\int (g - f) \psi_x \, du \, dv \, d\xi = 0, \tag{3}$$

at any point in space and time.

The BGK model was originally proposed to describe the essential physics of molecular interactions with τ chosen as the molecular collision time. Although the BGK model appears to describe only weak departures from local equilibria, it has long been recognized that such an approximation works well beyond its theoretical limits as long as the relaxation time is known for the physical process. Based on the above BGK model, the Navier–Stokes equations can be derived with the Chapman–Enskog expansion truncated to the 1st-order,

$$f = g + Kn f_1 = g - \tau(\partial g / \partial t + u \partial g / \partial x + v \partial g / \partial y). \tag{4}$$

For the Burnett and super-Burnett solutions, the above expansion can be naturally extended [21], such as $f = g + Kn f_1 + Kn^2 f_2 + Kn^3 f_3 + \dots$

Based on Eq. (4) and the BGK model for the continuum flow limit, the Navier–Stokes equations, the stress and Fourier heat conduction terms can be derived. The derived Navier–Stokes equations for the diatomic gas in the two-dimensional case can be written as,

$$\frac{\partial W}{\partial t} + \frac{\partial F}{\partial x} + \frac{\partial G}{\partial y} = \frac{\partial F_v}{\partial x} + \frac{\partial G_v}{\partial y}, \tag{5}$$

where

$$W = \begin{pmatrix} \rho \\ \rho U \\ \rho V \\ \rho E \end{pmatrix}, \quad F = \begin{pmatrix} \rho U \\ \rho U^2 + p \\ \rho UV \\ (\rho E + p)U \end{pmatrix}, \quad G = \begin{pmatrix} \rho V \\ \rho UV \\ \rho V^2 + p \\ (\rho E + p)V \end{pmatrix},$$

and

$$F_v = \begin{pmatrix} 0 \\ \tau p \left[2 \frac{\partial U}{\partial x} - \frac{2}{2+K} \left(\frac{\partial U}{\partial x} + \frac{\partial V}{\partial y} \right) \right] \\ \tau p \left(\frac{\partial U}{\partial y} + \frac{\partial V}{\partial x} \right) \\ \tau p \left[\left(U \left(2 \frac{\partial U}{\partial x} - \frac{2}{2+K} \left(\frac{\partial U}{\partial x} + \frac{\partial V}{\partial y} \right) \right) + V \left(\frac{\partial U}{\partial y} + \frac{\partial V}{\partial x} \right) \right) + \frac{K+4}{4} \frac{\partial}{\partial x} \left(\frac{1}{\lambda} \right) \right] \end{pmatrix},$$

and

$$G_v = \begin{pmatrix} 0 \\ \tau p \left(\frac{\partial U}{\partial y} + \frac{\partial V}{\partial x} \right) \\ \tau p \left[2 \frac{\partial V}{\partial y} - \frac{2}{2+K} \left(\frac{\partial U}{\partial x} + \frac{\partial V}{\partial y} \right) \right] \\ \tau p \left[\left(U \left(\frac{\partial U}{\partial y} + \frac{\partial V}{\partial x} \right) + V \left(2 \frac{\partial V}{\partial y} - \frac{2}{2+K} \left(\frac{\partial U}{\partial x} + \frac{\partial V}{\partial y} \right) \right) \right) + \frac{K+4}{4} \frac{\partial}{\partial y} \left(\frac{1}{\lambda} \right) \right] \end{pmatrix},$$

where $p = \rho/(2\lambda)$ is the pressure, $\rho E = (\rho/2)(U^2 + V^2) + ((K + 2)/2)p$ is the total energy density, and $\mu = \tau p$ is the dynamic viscosity coefficient. With the relation $\lambda = m/2kT$ and $C_p = 7k/2m$ for a diatomic gas, the heat conduction coefficient in the above equations becomes $\kappa = 7k\mu/2m$, and the Prandtl number becomes a fixed value $Pr = \mu C_p/\kappa = 1$. This is a well known result for the BGK model for both monatomic and diatomic gases. If the above viscous term is written in the standard NS formulation, the bulk viscosity term becomes

$$(2/3 - 2/(K + 2))\tau p(U_x + V_y) = (4/15)\tau p(U_x + V_y), \tag{6}$$

with $K = 3$ [31]. For the above Navier–Stokes solutions, the gas-kinetic BGK–NS scheme based on the kinetic BGK model has been well developed [28]. In this scheme, the Pr number is justified to any realistic value through the modification of heat flux through the cell interface. The accuracy of the scheme for the equilibrium NS equations are well demonstrated in the hypersonic viscous heat conducting flows [32].

2.2. Non-equilibrium rotational and translational temperature model

In the above Navier–Stokes equations, a single temperature is assumed for translational and rotational modes. Therefore, the bulk viscosity term appears. However, the simulation of non-equilibrium flow based on the bulk viscosity term is not successful in the rarefied flow regime. In the general case of non-equilibrium, temperature for the translational and rotational energy modes will be different. In this section, we are going to construct a non-equilibrium rotational energy relaxation model into the BGK equation and derive the corresponding macroscopic governing equations.

In general, the above-mentioned BGK model can be extended as the following:

$$\frac{\partial f}{\partial t} + u \frac{\partial f}{\partial x} + v \frac{\partial f}{\partial y} = \frac{f^{eq} - f}{\tau} + \frac{g - f^{eq}}{Z_r \tau} = \frac{f^{eq} - f}{\tau} + Q, \tag{7}$$

where for a diatomic gas an intermediate equilibrium state f^{eq} is introduced with two temperatures, one for translational and the other for rotational,

$$f^{eq} = \rho \left(\frac{\lambda_t}{\pi} \right)^{\frac{3}{2}} \left(\frac{\lambda_r}{\pi} \right) e^{-\lambda_t[(u-U)^2 + (v-V)^2 + w^2] - \lambda_r \xi_r^2}, \tag{8}$$

where ρ is the density, $\lambda_t = m/2kT_t$ is related to the translational temperature T_t , and $\lambda_r = m/2kT_r$ to the rotational temperature T_r . Therefore, the relaxation process becomes $f \rightarrow f^{eq} \rightarrow g$, and the process from f^{eq} to g takes a much longer time $Z_r\tau$ than that of translational equilibrium by τ . The nitrogen molecule has two rotational degrees of freedom $K_r = 2$, such that $\xi_r^2 = \xi_1^2 + \xi_2^2$. The additional term Q in the collision part is related to the relaxation between the translational and rotational non-equilibrium, which contributes to the source term for the macroscopic equations derived later. The above model is a special case of a generalized BGK model [30], which has the similarity with the two relaxation time BGK models for gases with internal degree of freedom [16,23].

The relation between mass ρ , momentum $(\rho U, \rho V)$, total energy ρE , and rotational energy ρE_r densities with the distribution function f is

$$W = \begin{pmatrix} \rho \\ \rho U \\ \rho V \\ \rho E \\ \rho E_r \end{pmatrix} = \int \psi f \, du \, dv \, dw \, d\xi_r,$$

where ψ has the components

$$\psi = \left(1, u, v, \frac{1}{2}(u^2 + v^2 + w^2 + \xi_r^2), \frac{1}{2}\xi_r^2 \right)^T.$$

In the above kinetic model, a new temperature λ_r is introduced. In order to self-consistently determine all unknowns, one more constraint has to be imposed on the kinetic model. This additional condition is the rotational energy relaxation. Since only mass, momentum and total energy are conserved during particle collisions, the compatibility condition for the collision term becomes,

$$\int \left(\frac{f^{eq} - f}{\tau} + Q \right) \psi_\alpha du dv dw d\xi_r = \mathbf{S} = (0, 0, 0, 0, s)^T, \quad \alpha = 1, 2, 3, 4, 5. \tag{9}$$

The source term for the rotational energy is due to the energy exchange between the translational and rotational ones. The format of this source term is modeled through the Landau–Teller–Jeans-type relaxation model, i.e.,

$$s = \rho(E_r^{eq} - E_r)/(Z_r\tau). \tag{10}$$

This source term cannot be derived from the BGK model itself. In other words, the above kinetic model is an extension of the traditional BGK model. To account for the longer relaxation time for the rotational energy to get equilibrium, the particle collision time τ is enlarged by a factor Z_r , the so-called rotational collision number. The equilibrium energy ρE_r^{eq} in the source term s is determined using the assumption $T_r = T_t = T$, such that

$$\rho E_r^{eq} = \rho/\lambda_r^{eq} \quad \text{and} \quad \lambda_r^{eq} = \frac{5}{4} \frac{\rho}{\rho E - \frac{1}{2}\rho(U^2 + V^2)}.$$

Using the BGK model with the thermodynamic state given in Eq. (8), and with the consideration that the relaxation from f to f^{eq} takes a much shorter time than that needed for translational and rotational equilibrium, with the frozen of rotational energy exchange the 1st-order Chapman–Enskog expansion gives,

$$f = f^{eq} + Knf_1 = f^{eq} - \tau(\partial f^{eq}/\partial t + u\partial f^{eq}/\partial x + v\partial f^{eq}/\partial y), \tag{11}$$

from which the corresponding macroscopic Navier–Stokes continuum equations in 2D case can be derived,

$$\frac{\partial W}{\partial t} + \frac{\partial F}{\partial x} + \frac{\partial G}{\partial y} = \frac{\partial F_v}{\partial x} + \frac{\partial G_v}{\partial y} + S, \tag{12}$$

where

$$W = \begin{pmatrix} \rho \\ \rho U \\ \rho V \\ \rho E \\ \rho E_r \end{pmatrix}, \quad F = \begin{pmatrix} \rho U \\ \rho U^2 + p \\ \rho UV \\ (\rho E + p)U \\ \rho E_r U \end{pmatrix}, \quad G = \begin{pmatrix} \rho V \\ \rho UV \\ \rho V^2 + p \\ (\rho E + p)V \\ \rho E_r V \end{pmatrix},$$

and

$$F_v = \begin{pmatrix} 0 \\ \tau_{xx} \\ \tau_{xy} \\ U\tau_{xx} + V\tau_{xy} + q_x \\ U\tau_{tr} + q_{rx} \end{pmatrix}, \quad G_v = \begin{pmatrix} 0 \\ \tau_{yx} \\ \tau_{yy} \\ U\tau_{yx} + V\tau_{yy} + q_y \\ V\tau_{tr} + q_{ry} \end{pmatrix},$$

where $\rho E = (1/2)\rho(U^2 + V^2 + 3RT_t + 2RT_r)$ is the total energy, $\rho E_r = \rho RT_r$ is the rotational energy. The pressure p is related to the translational temperature only through $p = \rho RT_t$. At the same time, the viscous and heat conduction terms are

$$\begin{aligned} \tau_{xx} &= \tau p \left[2 \frac{\partial U}{\partial x} - \frac{2}{3} \left(\frac{\partial U}{\partial x} + \frac{\partial V}{\partial y} \right) \right] - \frac{\rho K_r}{2(K_r + 3)} \frac{1}{Z_r} \left(\frac{1}{\lambda_t} - \frac{1}{\lambda_r} \right) \\ \tau_{yy} &= \tau p \left[2 \frac{\partial V}{\partial y} - \frac{2}{3} \left(\frac{\partial U}{\partial x} + \frac{\partial V}{\partial y} \right) \right] - \frac{\rho K_r}{2(K_r + 3)} \frac{1}{Z_r} \left(\frac{1}{\lambda_t} - \frac{1}{\lambda_r} \right) \\ \tau_{xy} &= \tau_{yx} = \tau p \left(\frac{\partial U}{\partial y} + \frac{\partial V}{\partial x} \right) \\ q_x &= \tau p \left[\frac{K_r}{4} \frac{\partial}{\partial x} \left(\frac{1}{\lambda_r} \right) + \frac{5}{4} \frac{\partial}{\partial x} \left(\frac{1}{\lambda_t} \right) \right], \\ q_y &= \tau p \left[\frac{K_r}{4} \frac{\partial}{\partial y} \left(\frac{1}{\lambda_r} \right) + \frac{5}{4} \frac{\partial}{\partial y} \left(\frac{1}{\lambda_t} \right) \right] \\ \tau_{rt} &= \frac{3\rho K_r}{4(K_r + 3)} \frac{1}{Z_r} \left(\frac{1}{\lambda_t} - \frac{1}{\lambda_r} \right) \\ q_{rx} &= \tau p \frac{K_r}{4} \frac{\partial}{\partial x} \left(\frac{1}{\lambda_r} \right), \end{aligned}$$

and

$$q_{ry} = \tau p \frac{K_r}{4} \frac{\partial}{\partial y} \left(\frac{1}{\lambda_r} \right).$$

The source term in Eq. (12) is given by

$$\mathbf{S} = \left(0, 0, 0, 0, \frac{\rho E_r^{\text{eq}} - \rho E_r}{Z_r \tau} \right), \tag{13}$$

and the value Z_r may depend on the temperature [14].

Instead of the bulk viscosity term in the standard NS Eq. (6), a relaxation term between translational and rotational energy is obtained in the above equations to model the non-equilibrium process. For example, the bulk viscosity term in the NS Eq. (5),

$$\frac{4}{15} \tau p (U_x + V_y)$$

is replaced by the temperature relaxation term in the above Eq. (12),

$$-\frac{\rho}{2Z_r} \frac{K_r}{K_r + 3} \left(\frac{1}{\lambda_t} - \frac{1}{\lambda_r} \right) = \frac{\rho R}{Z_r} \frac{K_r}{K_r + 3} (T_r - T_t),$$

where T_t and T_r are translational and rotational temperatures of the diatomic gas. In the limiting case of small departures from equilibrium, the rotational energy equation becomes

$$\frac{1}{Z_r \tau} \frac{3}{5} \rho R (T_t - T_r) = \frac{\partial}{\partial t} (\rho E_r) + \frac{\partial}{\partial x} (\rho U E_r) + \frac{\partial}{\partial y} (\rho V E_r),$$

and with the Euler approximation for the right hand side of the above equation, we have

$$T_t - T_r = -\frac{2}{3} Z_r \tau T (U_x + V_y),$$

and the normal bulk viscosity term can be exactly recovered, given by

$$\frac{\rho R}{Z_r} \frac{K_r}{K_r + 3} (T_r - T_t) = \frac{2}{3} \frac{K_r}{K_r + 3} \tau p (U_x + V_y),$$

where K_r is equal to 2 for two rotational degree of freedom. As shown in Section 4, the assumption of small temperature differences between translational and rotational modes is not valid in the non-equilibrium flow region, such as inside the shock layer or the hypersonic flow near isothermal boundary. Therefore, the above governing equations with a temperature relaxation term are more physically meaningful than the bulk

viscosity assumption. However, instead of solving the nonlinear system (12), the kinetic equation with the distribution function truncated up to the Navier–Stokes order (11) will be directly used in the numerical scheme for the solution of Eq. (12).

From the above relaxation model, we can realize that the bulk viscosity is not a physical property of a gas, but rather, an approximation designed to simulate the effect of thermal relaxation when the governing equations are cast in terms of a single temperature. This approximation is based on the assumption that the time scale of the macroscopic gas motion is much larger than the relaxation time for the rotational equilibrium. This is a good approximation only for low Knudsen number flows in the continuum flow regime. When the time scale for rotational relaxation is compatible with the characteristic time scale, the relaxation model needs to be used to account for the relaxation of rotational energy [15]. For the translation temperature below 1400 K in a nitrogen gas which is of interest here, the use of a single rotational temperature and the above Landau–Teller–Jeans model for rotational relaxation is adequate in the present study. The particle collision time multiplied by a rotational collision number Z_r models the relaxation process for the rotational energy to equilibrate with the translational energy. Determining the value of Z_r by theoretical and experimental means is an active research area [18] and is beyond the scope of the present work. In the current paper, the value Z_r used is

$$Z_r = \frac{Z_r^\infty}{1 + (\pi^{3/2}/2)\sqrt{T^*/T} + (\pi + \pi^2/4)(T^*/T)},$$

where the quantity T^* is the characteristic temperature of intermolecular potential, and Z_r^∞ is the limiting value. In a temperature range from 30 K to 3000 K for N_2 , the values $Z_r^\infty = 23.0$ and $T^* = 91.5$ K are used. The local temperature T in the above equation is equal to the translational temperature.

2.3. Generalization of particle collision time in rarefied flow regime

The definition of particle collision time is given by $\tau = \mu/p$, where μ is the dynamical viscosity coefficient. This definition of the particle collision time is coming from the connection between the kinetic model and macroscopic governing equations through the Chapman–Enskog expansion. In other words, this definition is validated in the continuum flow regime only, where the Chapman–Enskog expansion is appropriate. In the past two decades, the extended hydrodynamics approach for the non-equilibrium flow consisted of the inclusion of higher-order terms resulting in the Burnett or Super-Burnett equations, or regularizing the moment equations. But the success is limited. Currently, however, the most successful method to accurately match the experimental data for both monatomic and diatomic gases is the DSMC method. The DSMC method primarily consists of two steps, i.e., free transport and collision within each computational cell. The determination of the transport coefficients in the DSMC method is based on the particle collision model, which is actually constructed from the well-defined theories developed for continuum flow models. The collision models of the particle cross section and the probability for each collision pair can be used for recovering the dissipative coefficients in the Navier–Stokes limit. For example, the commonly used DSMC’s variable hard sphere (VHS) molecular model can be used to recover the 1st order Chapman–Enskog expansion with viscosity coefficient $\mu = \mu_{\text{ref}}(T/T_{\text{ref}})^\omega$. This is of the Navier–Stokes order. However, when the DSMC method is used in the non-equilibrium flow calculation, the particle transport from one place to another place is controlled individually by each particle’s velocity, which is not uniformly controlled by the macroscopically defined particle collision time, i.e., $\tau = \mu/p$. Therefore, the particle transport from one place to another place in the DSMC may be the core for the capturing of non-equilibrium properties. Hence, special attention has to be paid to the particle collision time, or the constitutive relationship, when using continuum formulation for rarefied flow computation. Traditionally, it is noted that the concepts and measurements of the dissipative coefficients are limited to the continuum flow regime. A generalized mathematical formulation of the stress and heat flux under rarefied flow conditions has not been developed so far. When we extend the continuum models to the non-equilibrium flow in the transition and rarefied regimes, we now face the need to figure out the effect of translational non-equilibrium, such as the new formulation of the particle collision time, and subsequently to determine the viscosity and heat conduction coefficients in these flows. This generalization must be based on the kinetic equation that is valid for

all flow regimes, and further, it is preferable to have a closed solution of the kinetic equation instead of a truncated expansion.

Our generalization of particle collision time is based on the existence of the closed solution of the BGK model [29], which is assumed to be

$$f = f^{eq} - \tau_*(\partial f^{eq}/\partial t + u\partial f^{eq}/\partial x + v\partial f^{eq}/\partial y), \tag{14}$$

where τ_* is the parameter to be determined. The difference between the above solution and the 1st-order Chapman–Enskog expansion (4) and (11) is that a generalized collision time τ_* is introduced. Substituting the above equation into the BGK model (1), we can obtain the relation between the generalized particle collision time τ_* and the collision time τ , which is well-defined in the continuum flow regime,

$$\tau_* = \frac{\tau(1 - D\tau_*)}{1 + \tau(D^2 f^{eq}/Df^{eq})}, \tag{15}$$

where $D = \partial/\partial t + u\partial/\partial x + v\partial/\partial y$. To the leading order, a simplified local collision time,

$$\tau_* = \frac{\tau}{1 + \tau(D^2 f^{eq}/Df^{eq})}, \tag{16}$$

is used in the computation in this paper. One of the main reason for the removal of $D\tau_*$ term is that τ_* is independent of particle velocity and any averaging of the random particle velocity trajectory is assumed to be zero. In the continuum flow regime, $\tau D^2 f^{eq}/Df^{eq} \sim Kn$, is expected to be small and τ_* reverts back to τ , determined from $\tau = \mu/p$. The dynamic viscosity coefficient μ can be obtained experimentally or theoretically as in Sutherland’s law. In order to remove the dependence of the collision time τ_* on the individual molecular velocity, $D^2 f^{eq}/Df^{eq}$ can be evaluated by taking moment ϕ , as $\int \phi D^2 f^{eq} du dv dw / \int \phi Df^{eq} du dv dw$, where $\phi_1 = (u - U)^2$. The reason to chose the above ϕ is that $(1, u, u^2)$ are the conservative moments for the translational motion, and the only term left, which is not conservative one, is ϕ . Since both $D^2 f^{eq}$ and Df^{eq} involve higher spatial and temporal derivatives of an equilibrium gas distribution function, a nonlinear limiter is imposed on the evaluation of τ^* ,

$$\tau_* = \frac{\tau}{1 + \max[-Kn, \tau \min((D^2 f^{eq}/Df^{eq}), Kn)]}, \tag{17}$$

where Kn is the Knudsen number of the flow problem.

3. Finite volume gas-kinetic method and kinetic boundary condition

3.1. Multiscale kinetic scheme

The continuum model developed in the previous section is solved based on the gas-kinetic BGK scheme [28]. It is a conservative finite volume method, and the numerical fluxes at cell interfaces are evaluated based on the time-dependent gas distribution function,

$$f = f^{eq} - \tau_*(\partial f^{eq}/\partial t + u\partial f^{eq}/\partial x + v\partial f^{eq}/\partial y) + t \frac{\partial f^{eq}}{\partial t}, \tag{18}$$

The relation between τ_* and τ is given in Eq. (17), where $\tau = \mu/p$ and μ is given by the Sutherland’s law.

In 2D case, for a diatomic gas the equilibrium state f^{eq} with translational and rotational temperature is

$$f^{eq} = \rho \left(\frac{\lambda_t}{\pi}\right)^{3/2} \left(\frac{\lambda_r}{\pi}\right)^{K_r/2} \exp\left(-\lambda_t((u - U)^2 + (v - V)^2 + w^2) - \lambda_r \xi_r^2\right), \tag{19}$$

where K_r is the rotational degree of freedom, i.e., $K_r = 2$. The expansion $\partial f^{eq}/\partial x$ can be expressed as

$$\frac{\partial f^{eq}}{\partial x} = \frac{1}{\rho} (a_1 + a_2 u + a_3 v + a_4 (u^2 + v^2 + w^2) + a_5 \xi_r^2) f^{eq} = \frac{1}{\rho} a f^{eq}.$$

Here, all the coefficients can be explicitly determined by relating the microscopic and macroscopic variables at the cell interface, i.e., $W = \int \psi f^{eq} du dv dw d\xi_r$ and $\partial W/\partial x = (1/\rho) \int \psi a f^{eq} du dv dw d\xi_r$, where $W = (\rho, \rho U, \rho V, \rho E, \rho E_r)^T$ are the macroscopic flow variables.

With the defined variables,

$$B = 2 \frac{\partial(\rho E - \rho E_r)}{\partial x} - (U^2 + V^2 + \frac{3}{2\lambda_t}) \frac{\partial \rho}{\partial x},$$

$$A_1 = \frac{\partial(\rho U)}{\partial x} - U \frac{\partial \rho}{\partial x},$$

$$A_2 = \frac{\partial(\rho V)}{\partial x} - V \frac{\partial \rho}{\partial x},$$

we have

$$a_5 = 2 \frac{\lambda_r^2}{K_r} \left(2 \frac{\partial(\rho E_r)}{\partial x} - \frac{1}{2} \frac{K_r}{\lambda_r} \frac{\partial \rho}{\partial x} \right),$$

$$a_4 = \frac{2\lambda_t^2}{3} (B - 2UA_1 - 2VA_2),$$

$$a_3 = 2\lambda_t A_2 - 2Va_4,$$

$$a_2 = 2\lambda_t A_1 - 2Ua_4,$$

$$a_1 = \frac{\partial \rho}{\partial x} - a_2 U - a_3 V - a_4 \left(U^2 + V^2 + \frac{3}{2\lambda_t} \right) - a_5 \frac{K_r}{2\lambda_r}.$$

The temporal variation of $\partial f^{\text{eq}}/\partial t$ can be expanded similarly as a spatial expansion and the corresponding coefficients can be obtained from the compatibility condition for the Chapman–Enskog expansion, i.e.,

$$\int \psi (\partial f^{\text{eq}}/\partial t + u \partial f^{\text{eq}}/\partial x + v \partial f^{\text{eq}}/\partial y) du dv dw d\xi_r = 0,$$

where the above five equations uniquely determine the five unknowns in A , i.e., $A = A_1 + A_2 u + A_3 v + A_4(u^2 + v^2 + w^2) + A_5 \xi_r^2$.

The numerical method developed for Eq. (12) is a finite volume method,

$$\mathbf{W}_{i,j}^{n+1} = \mathbf{W}_{i,j}^n + \frac{1}{\Delta V} \sum_{l=1}^{l=4} \int_0^{\Delta t} \mathbf{F}_l \cdot \mathbf{n}_l \Delta S_l dt + \mathbf{S}_{i,j}^n \Delta t, \quad (20)$$

where $\mathbf{W}_{i,j}^n$ is the cell averaged mass, momentum, total energy, and rotational energy, and \mathbf{F}_l are the corresponding fluxes through interface l with length scale ΔS_l of the control volume (i, j) . The volume of the numerical cell (i, j) is ΔV . The fluxes across the cell interface are evaluated using the solution (18),

$$\mathbf{F} = \int \tilde{u} \psi f du dv dw d\xi,$$

where the \tilde{u} is the particle velocity in the normal direction of the cell interface. Note that Δt is the time step $\Delta t = t^{n+1} - t^n$, and $\mathbf{S}_{i,j}^n$ is the source term for the rotational energy, given in Eq. (13). The main difference between the current non-equilibrium kinetic method and the equilibrium BGK–NS method in [28] is that two temperatures T_t and T_r are used with a generalized particle collision time τ_* . In order to simulate the flow with any realistic Prandtl number, a modification of the heat flux in the energy transport, such as that used in [28], is also implemented in the present study.

3.2. Gas-kinetic boundary condition

The interaction between the gas flow and the solid boundary has been explicitly pointed out by many authors, see [19,7]. This section is mainly about how to implement these ideas numerically in the current gas-kinetic scheme for non-equilibrium flow.

For the flows in the near continuum regime, even for the Navier–Stokes equations the application of slip boundary condition becomes necessary. Since the gas-kinetic BGK-type schemes are based on the time evo-

lution of gas distribution function to update the flow variables, the slip boundary condition can be naturally obtained in the kinetic method.

In the slip flow regime, with the one-sided interpolation of the flow variables up to the wall, we can use the same technique presented in the last section to evaluate the gas distribution function f^{in} there, see Eq. (18). Therefore, we can evaluate the total number of particles hitting on the wall $\int_0^{\Delta t} \int_{u<0} u f^{\text{in}} du dv dw d\xi_r dt$. All these particles will be reflected from the wall according to the specular reflection coefficient β . With the assumption of wall temperature T_w , i.e., $\lambda_w = m/(2kT_w)$, we can construct an equilibrium state there first, i.e.,

$$g^w = \rho_w \left(\frac{\lambda_w}{\pi}\right)^{\frac{3}{2}} e^{-\lambda_w(u^2+v^2+w^2)} \left(\frac{\lambda_{wr}}{\pi}\right)^{\frac{K_r}{2}} e^{-\lambda_{wr}\xi_r^2},$$

where the temperature of the rotational degree of freedom λ_{wr} may not be the same as the wall temperature λ_w . A single particle collision with the wall may not change the particle rotational temperature. Therefore, one choice of the wall rotational temperature is to keep the rotational temperature of incoming molecules. In the above equilibrium state, the solid wall is assumed to be stationary. The requirement of no particles penetrating through the wall is equivalent to

$$\int_0^{\Delta t} \int_{u>0} u g^w du dv dw d\xi_r dt = - \int_0^{\Delta t} \int_{u<0} u f^{\text{in}} du dv dw d\xi_r dt,$$

from which the density ρ_w in g^w can be obtained

$$\rho_w = - \frac{2\sqrt{\pi\lambda_w}}{\Delta t} \int_0^{\Delta t} \int_{u<0} u f^{\text{in}} du dv dw d\xi_r dt.$$

Therefore, the total gas distribution function at the wall for the accommodation coefficient ($\sigma = 1 - \beta$) can be written as

$$f^{\text{total}} = (1 - \beta)g^w_{u>0} + f^{\text{in}}_{u<0} + \beta f^{\text{in}}_{u<0}(-u, v),$$

where the term $\beta f^{\text{in}}_{u<0}(-u, v)$ accounts for the component with specular reflection from the surface. In the case of no specular reflection, such as the fully accommodation case $\sigma = 1$, β is equal to 0. In all our calculations in this paper, $\sigma = 1$ is used. After obtaining the gas distribution function f^{total} at the wall, the flux across the solid boundary can be evaluated in the same way as Eq. (18). The slip boundary condition forms automatically from f^{total} in the gas-kinetic BGK scheme, such as the slip velocity

$$V_{\text{slip}} = \frac{\int v f^{\text{total}} du dv dw d\xi_r}{\int f^{\text{total}} du dv dw d\xi_r} \neq 0,$$

along the solid surface. Also, the averaged temperature of f^{total} will be different from the wall temperature and the temperature slip can be obtained automatically.

4. Non-equilibrium flow computations

In an early paper, the multiple temperature model in 1D case has been developed and tested for both argon and nitrogen shock structures [31]. Besides the good match in density and temperature distributions between the experimental data and the current multiple temperature results, the stress and heat flux have also been compared with the Boltzmann and DSMC solutions [20,4]. In this section, we are going to test the current 2D model and its kinetic scheme to two cases of a 3D axis-symmetric nozzle flow and a 2D hypersonic flow over a flat plate [9,26]. In both cases, the extrapolation is used for the outlet boundary condition on the right. The experimental measurements of the rotational temperature are available for both cases.

4.1. Low-density nozzle flow

The mission performance of satellites and spacecrafts such as on-orbit lifetimes, and trip times are significantly impacted by low-thrust rocket engines that are used for the control of altitude and trajectory of the

vehicle. The understanding of the detailed flow structure inside low-thrust rocket nozzles is very important for the accurate prediction of the thrust and mass flow levels, and also for the precise analysis of the plume and backflow. For this type of rocket engine, due to the small thrust level, nozzle scales are quite small and reservoir pressure are very low. Reynolds number of the flow in the nozzle are very low and rarefaction effects can significantly alter the internal flow structure in the vacuum of the space environment. Under these conditions, the gas exhibits strong non-equilibrium effects, such as slip at the wall, due to rapid expansion into the low-density environment. The fluid experiences continuum, transition, and free molecular flow regime. Consequently, conventional continuum gas dynamics that are based on the concept of local equilibrium may not be adequate. Currently, the approach based on the molecular gas dynamics, such as DSMC method, is the only method for the analysis of the flow. The current gas-kinetic method is much more efficient than the DSMC method for high and normal density flows. Thus, the test of the validity of the current method in the rarefied flow regime is necessary.

Few experimental data are available for this type of low-thrust nozzle. Rothe's experiment was probably the only one in which detailed low density flow properties of nitrogen have been measured inside a nozzle using the electron beam fluorescence technique [22]. This is an axis-symmetric flow problem. Both NS and

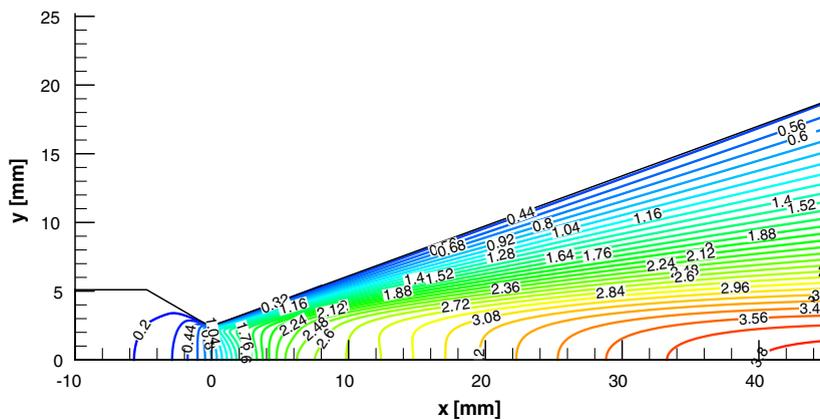


Fig. 1. Mach contours in the nozzle flow computations for the case with stagnation pressure $P_0 = 474$ Pa. 265×71 mesh points are used in the whole domain.

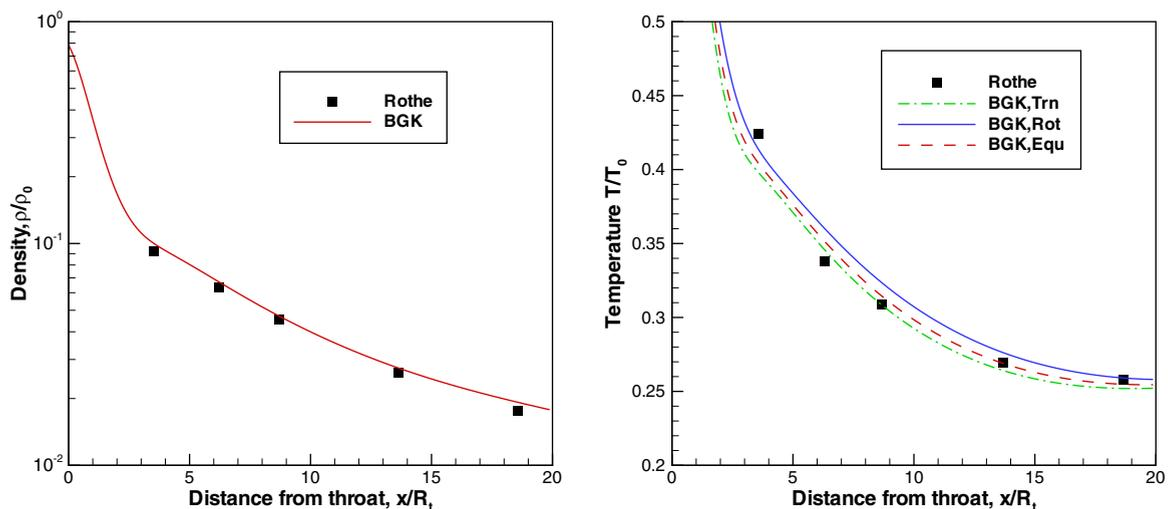


Fig. 2. Density and temperature distributions along the central line of the nozzle, where R_t is the throat radius. The measured rotational temperature is from Rothe's experiment [22].

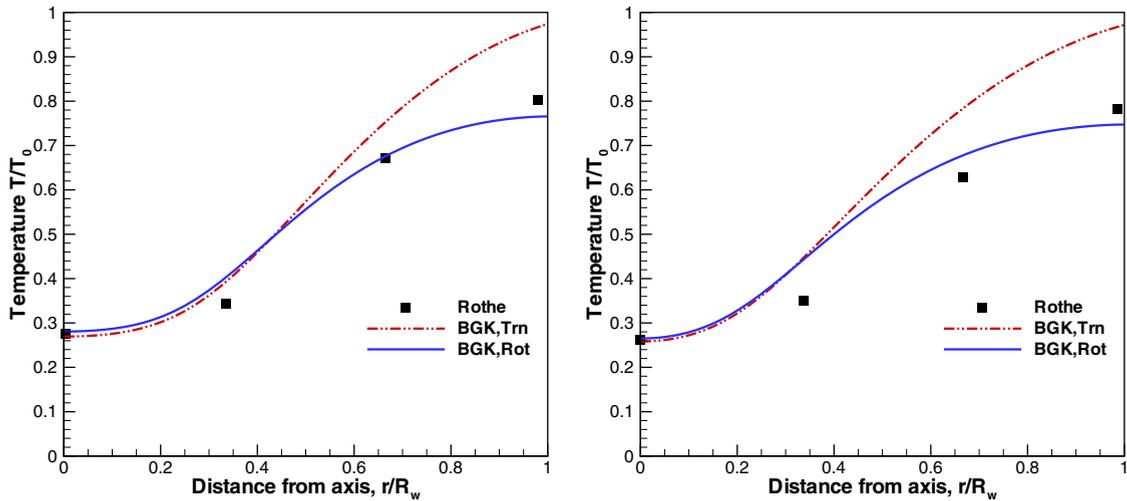


Fig. 3. Temperature distributions at locations $x/R_t = 13.7$ (left figure) and $x/R_t = 18.7$ (right figure) in the nozzle cross section direction, where R_t is the throat radius.

DSMC simulations of the internal nozzle flow have been performed by Chung et al. [9]. To evaluate the accuracy of the current method, we perform the simulation in the region of both inside and beyond the nozzle throat, where both equilibrium and non-equilibrium flows are simulated using the same method. Following the flow condition given by Chung et al. [9], the geometry and Mach contours are shown in Fig. 1, where 261×71 non-uniform mesh points are used inside the nozzle. The radius of curvature at the thrust is one half the throat radius of 2.55 mm. The nozzle divergence angle is 20° , the exit to throat area ratio is 66. The flow condition for the first test case is: stagnation temperature $T_0 = 300$ K, stagnation pressure $P_0 = 474$ Pa, wall temperature $T_w = 300$ K, and the Knudsen number $Kn = 2.3 \times 10^{-3}$. Figs. 1–3 show the results of computation and experimental data for Mach contour, density and temperature along the nozzle centerline, and the temperature profiles along the nozzle cross section at two locations $x = 137$ mm and $x = 187$ mm. With the same nozzle geometry, the second test has a different stagnation pressure, which is equal to $P_0 = 209$ Pa. The Mach contour inside the nozzle is shown in Fig. 4. The rotational, translational, and average temperatures, as well as experimental data for the rotational temperature along nozzle centerline is shown in Fig. 5. Excellent match in the rotational temperatures between the experiment and computation is obtained. However, in comparison with the DSMC results [9], there is obvious differences. For example, it is observed that the current model presents a cross point between the translational and rotational temperatures around

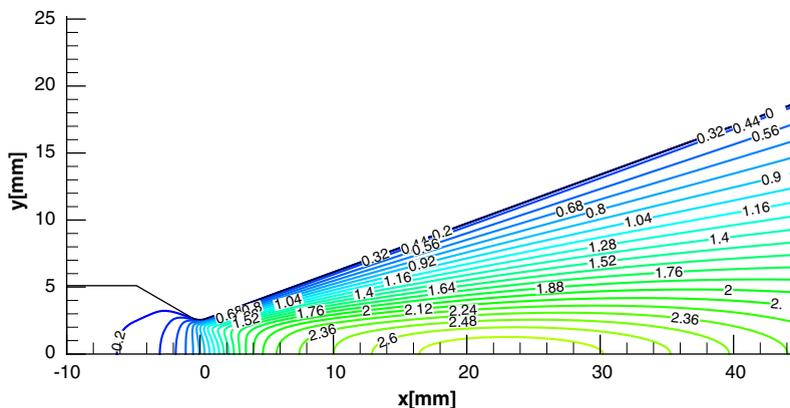


Fig. 4. Mach contour for the same case as previous one except low stagnation pressure of the incoming gas, i.e., $P_0 = 209$ Pa.

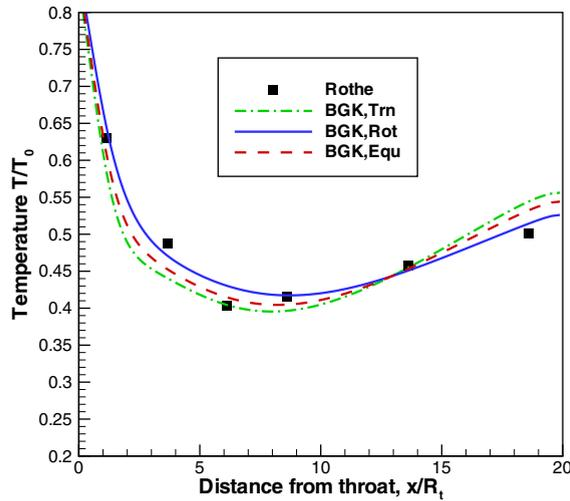


Fig. 5. Temperature distributions for the case with $P_0 = 209$ Pa. Rothe's experiment data is the measured rotational temperature.

$x = 14R_t$. But, this phenomenon has never been observed in the DSMC computation [9], where the rotational and translational temperatures move downward without crossing each other. The discrepancies in the simulation results can be only resolved with the help of experiments.

4.2. Rarefied hypersonic flow over a flat plate

Space vehicles, space stations, and planetary exploration systems, which have been developed recently, fly partly in a rarefied gas environment. Their velocity is hypersonic, and their flight environment include shock shock interactions and shock boundary interactions that cause high heat transfer and pressure on the body of the spacecraft. It is important that the physical phenomena occurring around spacecraft in a hypersonic rarefied gas flow are studied in detail in order to understand these phenomena and to design a real size vehicle.

Here following Tsuboi and Matsumoto's experiment [26], we are going to simulate the hypersonic rarefied gas flow over a flat plate, and compare our simulation results with the experimental measurements and DSMC solutions in [26]. The case we will study is the run 34, where the nozzle exit Mach number is 4.89, stagnation temperature $T_0 = 670$ K, stagnation pressure $P_0 = 983$ Pa, nozzle exit temperature $T_e = 116$ K, and flat plate surface temperature is 290 K. The geometric configuration is shown in Fig. 6, where 241×101 mesh points

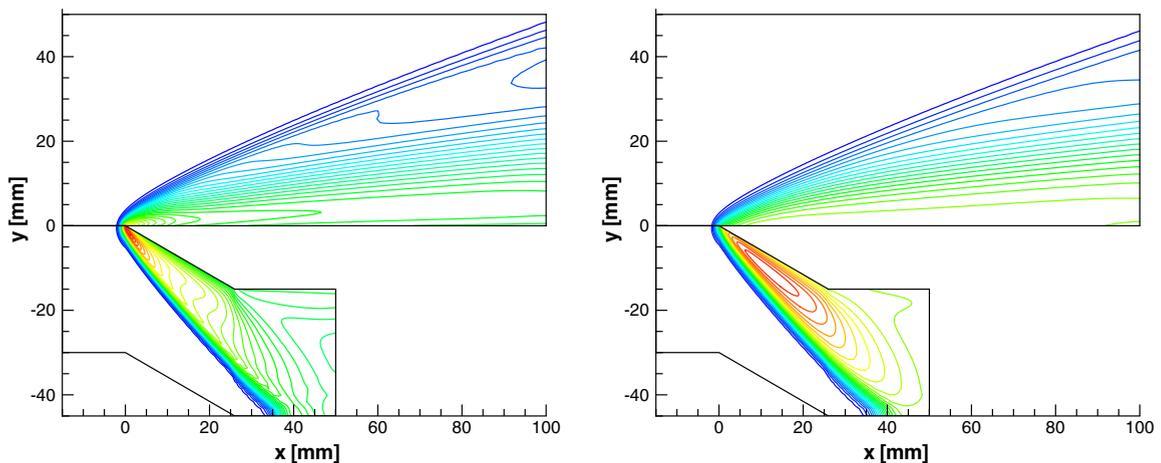


Fig. 6. Translational (left) and rotational (right) temperature contours in the hypersonic flow over a flat plate. 241×101 and 151×61 grid points are used above and below the flat plate.

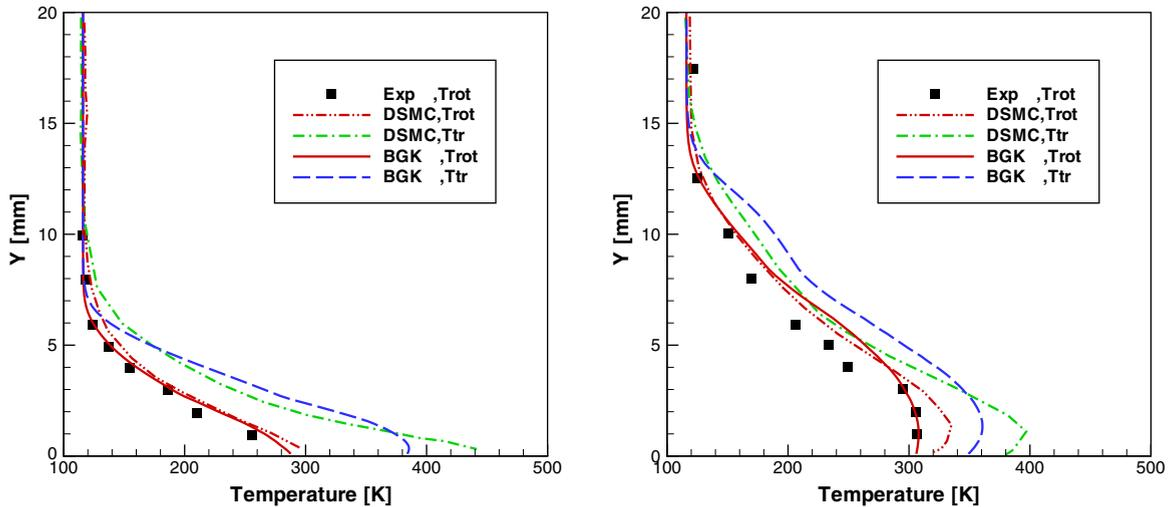


Fig. 7. Translational and rotational temperature distributions in the vertical direction at $x = 5$ mm (left) and $x = 20$ mm (right). The measured rotational temperature, DSMC solution [26], and the current BGK solutions are presented.

above the flat plate and 151×61 mesh points below the flat plate are used. In this case, the shock wave and boundary layer interaction near a sharp leading edge in a merged layer causes non-equilibrium between translational and rotational temperatures in the rarefied gas regime. A merged layer is defined as the mutual interaction between the external flowfield and the boundary layer growth around a body of given shape. In the experiment, the non-equilibrium rotational temperature distributions around sharp edged flat plate in a hypersonic rarefied gas flow exhausted from a converging–diverging nozzle were measured by an electron beam fluorescence technique. Fig. 6 presents the translational and rotational temperature contours around the sharp edged flat plate. The temperature distributions in the vertical direction above the flat plate at the locations of $x = 5$ mm and 20 mm from the leading edge are shown in Fig. 7. As a comparison, the DSMC results from Tsuboi and Matsumoto’s computation is also included [26]. As shown in Fig. 7, especially at the downstream location $x = 20$ mm, our computation results above the flat plate have a closer match with the experimental measurement than the DSMC solution. In the DSMC solution, the rotational temperature profile above the flat plate is much curved.

5. Conclusion

In this paper, a continuum gas-kinetic formulation for the translational and rotational non-equilibrium flow is constructed. Based on the extended relaxation BGK kinetic model, the macroscopic governing equations for diatomic gas are derived, where the bulk viscosity term in the traditional Navier–Stokes equations are substituted by the temperature relaxation term. Also, in order to capture the transport non-equilibrium effect, a generalized constitutive relationships through the modification of particle collision time is used. Based on the newly developed multiple temperature kinetic model, a corresponding gas-kinetic scheme is constructed and used in the near continuum flow computations, where both nozzle flows and hypersonic rarefied flow over a flat plate are tested. The comparisons among the numerical solutions from the current kinetic model, the DSMC solutions, and experimental measurements provide confidence on the current kinetic model and its numerical method. Besides the DSMC method, the current kinetic method provides another effective alternative method for the study of flow motion in the near continuum and transition regimes. Since the current finite volume gas-kinetic scheme implements a continuous gas distribution function in the phase space, the fluxes for the macroscopic variables can be evaluated explicitly and efficiently. Also, the current method goes back to the Navier–Stokes flow solver automatically in the continuum flow regime when Knudsen number is very small. The temperature relaxation terms will go back to the bulk viscosity terms in the standard Navier–Stokes equations. So, the current method is a unified numerical method from continuum to near continuum flow regime.

Along with the shock structure calculations [31], and the test cases in the current paper, the validity of the multiple temperature kinetic model and its numerical method is confirmed.

Acknowledgments

We would like thank reviewers for their helpful comments. This research was supported by Hong Kong Research Grant Council HKUST6210/05E, 6214/06E, and the Croucher Foundation.

References

- [1] V.V. Aristov, Direct Methods for Solving the Boltzmann Equation and Study of Non-equilibrium Flows, Kluwer Academic Publishers, 2001.
- [2] P.L. Bhatnagar, E.P. Gross, M. Krook, A model for collision processes in gases. I: Small amplitude processes in charged and neutral one-component systems, *Phys. Rev.* 94 (1954) 511–525.
- [3] R. Balakrishnan, R.K. Agarwal, K.Y. Yun, BGK–Burnett equations for flows in the continuum-transition regime, *J. Thermophys. Heat Treat.* 13 (1999) 397–410.
- [4] G.A. Bird, Aspects of the structure of strong shock waves, *Phys. Fluids* 13 (1970) 1172–1177.
- [5] G.A. Bird, *Molecular Gas Dynamics and the Direct Simulation of Gas Flows*, Clarendon Press, Oxford, 1994.
- [6] A.V. Bobylev, The Chapman–Enskog and Grad methods for solving the Boltzmann equation, *Sov. Phys. Dokl.* 27 (1982) 29.
- [7] C. Cercignani, *Rarefied Gas Dynamics*, Cambridge University Press, 2000.
- [8] S. Chapman, T.G. Cowling, *The Mathematical Theory of Non-uniform Gases*, Cambridge University Press, 1990.
- [9] C.H. Chung, S.C. Kim, R.M. Stubbs, K.J. De Witt, Low-density nozzle flow by the direct simulation Monte Carlo and continuum methods, *J. Propulsion Power* 11 (1995) 64–70.
- [10] H. Grad, On the kinetic theory of rarefied gases, *Commun. Pure Appl. Math.* 2 (1949) 331–407.
- [11] M.S. Ivanov, S.F. Gimelshein, Computational hypersonic rarefied flows, *Annu. Rev. Fluid Mech.* 30 (1998) 469–505.
- [12] S. Jin, L. Pareschi, M. Slemrod, A relaxation scheme for solving the Boltzmann equation based on Chapman–Enskog expansion, *Acta Math. Appl. Sin. (Eng. Ser.)* 18 (2002) 37.
- [13] V.I. Kolobov, R.R. Arslanbekov, V.V. Aristov, A.A. Frolova, S.A. Zabelok, Unified solver for rarefied and continuum flows with adaptive mesh and algorithm refinement, *J. Comput. Phys.* 223 (2007) 589.
- [14] J.A. Lordi, R.E. Mates, Rotational relaxation in nonpolar diatomic gases, *Phys. Fluids* 13 (1970) 291–308.
- [15] F.E. Lumpkin III, Development and evaluation of continuum models for translational–rotational non-equilibrium, Ph.D. Thesis, Stanford University, 1990.
- [16] T.F. Morse, Kinetic model for gases with internal degrees of freedom, *Phys. Fluids* 7 (2) (1964) 159–169.
- [17] I. Muller, T. Ruggeri, Rational extended thermodynamics, *Springer Tracts in Natural Philosophy*, 37, Springer-Verlag, 1998.
- [18] C. Park, Rotational relaxation of N₂ behind a strong shock wave, *AIAA* 2002-3218, 2002.
- [19] G.N. Patterson, *Molecular Flow of Gases*, Wiley, New York, 1956.
- [20] T. Ohwada, Structure of normal shock waves: direct numerical analysis of the Boltzmann equation for hard-sphere molecules, *Phys. Fluids A* 5 (1993) 217–234.
- [21] T. Ohwada, K. Xu, The kinetic scheme for full Burnett equations, *J. Comput. Phys.* 201 (2004) 315–332.
- [22] D.E. Rothe, Electron beam studies of viscous flow in supersonic nozzles, *AIAA J.* 9 (1971) 804–811.
- [23] H. Struchtrup, The BGK model for an ideal gas with an internal degree of freedom, *Transp. Theory Stat. Phys.* 28 (4) (1999) 369–385.
- [24] H. Struchtrup, M. Torrilhon, Regularization of Grad’s 13 moment equations: derivation and linear analysis, *Phys. Fluids* 15 (2003) 2668–2680.
- [25] M. Torrilhon, H. Struchtrup, Regularized 13-moment-equations: shock structure calculations and comparison to Burnett models, *J. Fluid Mech.* 513 (2004) 171–198.
- [26] N. Tsuboi, Y. Matsumoto, Experimental and numerical study of hypersonic rarefied gas flow over flat plates, *AIAA J.* 43 (2005) 1243–1255.
- [27] W. Weiss, Continuous shock structure in extended thermodynamics, *Phys. Rev. E* 52 (1995) R5760–R5763.
- [28] K. Xu, A gas-kinetic BGK scheme for the Navier–Stokes equations and its connection with artificial dissipation and Godunov method, *J. Comput. Phys.* 171 (2001) 289–335.
- [29] K. Xu, Regularization of the Chapman–Enskog expansion and its description of shock structure, *Phys. Fluids* 14 (2002) L17.
- [30] K. Xu, A generalized Bhatnagar–Gross–Krook model for non-equilibrium flows, *Phys. Fluids* 20 (2008) 026101.
- [31] K. Xu, E. Josyula, Continuum formulation for non-equilibrium shock structure calculation, *Commun. Comput. Phys.* 1 (2006) 425–450.
- [32] K. Xu, M.L. Mao, L. Tang, A multidimensional gas-kinetic BGK scheme for hypersonic viscous flow, *J. Comput. Phys.* 203 (2005) 405–421.
- [33] X. Zhong, R.W. MacCormack, D.R. Chapman, Stabilization of the Burnett equations and application to hypersonic flows, *AIAA J.* 31 (1993) 1036–1043.